Original Article

Placental mesenchymal stem cell-derived interleukin-6 promotes neuroblastoma progression

Ying Liu, Bai Li, Huixia Wei, Yan Xu, Yufeng Liu

Department of Hematology and Oncology, Children's Hospital, The First Affiliated Hospital of Zhengzhou University, Zhengzhou 450052, Henan, P. R. China

Received May 14, 2025; Accepted July 24, 2025; Epub August 25, 2025; Published August 30, 2025

Abstract: Neuroblastoma (NB) is a prevalent pediatric malignancy, yet the role of mesenchymal stem cells (MSCs) in NB progression remains unclear. MSCs are known to secrete various cytokines, including interleukin (IL)-6, and their influence on NB cells and tumor xenografts were investigated in this study. Placenta-derived mesenchymal stem cells (PMSCs) were isolated from chorionic villi and characterized via flow cytometry. The obtained PMSCs were co-cultured with NB cells or IL-6-silenced PMSCs. Comprehensive assays were conducted to assess proliferation, colony formation, cell cycle progression, apoptosis, migration, invasion, and epithelial-mesenchymal transition (EMT). RNA-seq identified differentially expressed genes (DEGs) in NB cells, predominantly enriched in Janus kinase/signal transducer and activator of transcription (JAK/STAT) pathways (P < 0.05). qRT-PCR revealed elevated levels of IL-6 and other oncogenic cytokines in PMSCs (P < 0.05). In vivo, IL-6 knockdown in PMSCs significantly suppressed NB xenograft growth, accompanied by reduced expression of Ki-67, proliferating cell nuclear antigen (PCNA), Caspase 9, and Snail as shown by immunohistochemistry (P < 0.05). Western blotting confirmed activation of phosphatidylinositol 3-kinases/protein kinase B (PI3K/AKT) pathway in NB cells after co-culture with PMSCs, which was attenuated by PI3K inhibition. Notably, IL-6 knockdown markedly suppressed NB xenograft progression and downregulated associated signaling markers (P < 0.05). Collectively, PMSC-derived IL-6 potentiates NB progression via PI3K-AKT signaling, presenting a potential therapeutic target in neuroblastoma.

Keywords: Placental mesenchymal stem cells, neuroblastoma, interleukin-6, JAK/STAT pathway, PI3K-AKT pathway

Introduction

Neuroblastoma (NB) is an embryonal tumor primarily composed of undifferentiated neuroblasts [1]. It is the third most common pediatric malignancy, following brain tumors and leukemia, occupying 6-10% of childhood tumors [2]. NB is characterized by marked biological and clinical multiple heterogeneity [3-6], and is frequently diagnosed at an advanced stage, rendering many cases inoperable or difficult to cure. Treatment strategies vary depending on disease severity, and a subset of patients remains refractory to therapy. In advanced cases, chemotherapy, radiotherapy, immunotherapy, and stem cell transplantation remain critical remedies [7-9]. Despite multidisciplinary approaches, no universally effective therapeutic strategy has been established for clinical application.

Mesenchymal stem cells (MSCs) show unique therapeutic potential for various diseases due to their chemotactic properties and capacity to migrate to tumor sites [10, 11]. Because MSCs can interact with tumor cells, they have been used as carriers of anti-cancer genes, demonstrating promising anti-tumor effects in several cancer models [12]. Nonetheless, the precise mechanisms governing MSC-cancer cell interplay remain to be fully elucidated. By secreting an array of cytokines, MSCs can modulate cancer cell phenotypes, thereby influencing tumor initiation, progression, and metastasis [13-16]. Notably, placenta-derived MSCs (PMSCs) exhibit a longer lifespan and higher growth capacity compared to MSCs from other sources [17], potentially offering an advantageous resource for stem cell therapies. Despite numerous reports on the role of MSCs in different tumors. whether exogenous MSCs promote or inhibit

tumor growth remains controversial. Accordingly, clarifying the interaction between MSCs and NB cells is essential.

Interleukin (IL)-6 plays a pivotal role in chronic inflammatory diseases, autoimmune diseases, cancers, and cytokine- mediated disorders [18]. MSCs secrete a wide range of bioactive molecules that can promote cancer cell proliferation, angiogenesis, and invasiveness within the tumor microenvironment [19]. For example, MSCs-derived tenascin-C has been associated with breast cancer metastasis to lung tissues [20]. In this study, we investigated the biological characteristics of NB, assessed IL-6 expression levels in PMSCs, and further evaluated the effects of IL-6 on the NB cell behavior and PMSC-influenced tumor growth, alongside the underlying molecular mechanism. These findings contribute to our understanding of how PMSCs regulate NB progression and may inform the development of novel therapeutic strategies.

Materials and methods

Tissue harvest and cell culture

PMSCs were isolated from placentas obtained from healthy women who underwent full-term deliveries (38-40 weeks of gestation) without pregnancy complications. This study was approved by the Ethics Committee of Children's Hospital, The First Affiliated Hospital of Zhengzhou University (No. 2023-KY-1309). All experiments were carried out in accordance with the Declaration of Helsinki, and informed consent was obtained all patients.

Each placenta was processed within 2 hours postpartum. Following confirmation of normal gross morphology, the fetal side (chorionic villi) of the placentas was dissected under sterile conditions. The villi were carefully excised, rinsed with Hanke's balanced salt solution to remove blood clots, and then enzymatically digested with collagenase type I to release PMSCs [21]. The digested suspension was filtered and centrifuged to collect PMSCs, which were then cultured in Dulbecco's Modified Eagle's Medium/Nutrient Mixture F-12 (DMEM/F-12) supplemented with 10% fetal bovine serum (FBS) (PM150312A, Procell, Wuhan, China) and 1% antibiotics, and maintained at 37°C in a 5% CO₂ atmosphere.

Human NB cells (SK-N-SH and SK-N-MC), purchased from Procell (Wuhan, China), were cultured in DMEM (PM150220B, Procell, Wuhan, China) containing 10% FBS and 1% antibiotics under 5% CO₂ at 37°C. Short tandem repeat (STR) profiling and mycoplasma assay were performed to ensure the quality of both PMSCs cells and NB cells.

Lentivirus transduction

For IL-6 knockdown, PMSCs were transduced with a lentiviral short hairpin RNA (sh-IL-6) targeting IL-6, with sh-Con serving as the negative control. PMSCs were infected with sh-IL-6 or sh-Con in the presence of polybrene (Hanheng, Shanghai, China). The shRNA sequences were as follows: sh-IL-6-F, 5'-CCGGGCCAGATCATTTC-TTGGAAAGCGAACTTTCCAAGAAATGATCTGGCT-TTTTTG-3'; sh-IL-6-R, 5'-AATTCAAAAAAGCCAGATCATTTCTTGGAAAGTTCGCTTTCCAAGAAATGATCTGGC-3'; sh-Con, 5'-CAACAAGATGAAGAGCACCAA-3'.

Flow cytometry analysis of PMSCs surface markers

To characterize PMSCs, flow cytometry was performed to assess specific surface markers. After isolation from chorionic villi, live PMSCs were harvested using TrypLE Express enzyme, washed with PBS, and re-suspended in FACS buffer (0.5% BSA, 0.5% FBS, 1×PBS). The cells were then fixed sequentially in 50% and 100% methanol for 20 min each, followed by incubation in a cold blocking buffer (0.5% BSA, 2% FBS, 1×PBS) for 20 min. Antibodies CD90 (98126-1-RR, Proteintech, Wuhan, China), CD105 (98013-2-RR, Proteintech, Wuhan, China), CD144 (98071-1-RR, Proteintech, Wuhan, China), CD166 (DF7736, Proteintech, Wuhan, China), HLA-DR (FITC-65560, Proteintech, Wuhan, China), CD14 (FITC-65172, Proteintech, Wuhan, China) were then added into cell suspension and incubated for 35 min. Finally, 10,000 cells were gated for marker expression using a flow cytometer.

Western blot

Total protein was extracted using radioimmunoprecipitation assay (RIPA) buffer (R0010, Solarbio, Beijing, China) and quantified with a BCA Kit (P0010S, Beyotime, Shanghai, China). Equal amounts of protein (20 μ g) were sepa-

rated on 10% sodium dodecyl sulfate polyacrylamide gel electrophoresis (SDS-PAGE) and later transferred onto polyvinylidene fluoride (PVDF) membrane (YA1700, Solarbio, Beijing, China). Afterwards, the membranes were blocked with 5% fat-free milk for 60 min at room temperature and then incubated overnight at 4°C with the following primary anti bodies: IL-6 (Affinity, Lot. DF6087), PCNA (Lot. 10205-2-AP, Proteintech, Wuhan, China), caspase 9 (Lot. db21445, diagbio, Hangzhou, China), metalloproteinase (MMP)-1 (10371-2-AP, Proteintech, Wuhan, China), MMP-7 (10374-2-AP, Proteintech, Wuhan, China), N-cadherin (22018-1-AP, Proteintech, Wuhan, China), E-cadherin (20874-1-AP, Proteintech, Wuhan, China), Vimentin (10366-1-AP, Proteintech, Wuhan, China), Snail (13099-1-AP, Proteintech, Wuhan, China), p-JAK2 (AF3024, Affinity, Liyang, China), p-STAT1 (AF3300, Affinity, Liyang, China), p-PI3K (AF3241, Affinity, Liyang, China), p-AKT (AF8357, Affinity, Liyang, China), JAK2 (AF6022, Affinity, Liyang, China), STAT1 (AF6300, Affinity, Liyang, China), PI3K (db951, diagbio, Hangzhou, China), AKT (db1607, diagbio, Hangzhou, China), Ki-67 (GB111499, Servicebio, Wuhan, China). After washing, membranes were incubated with HRP-conjugated secondary antibody (ab6721, 1:5000, Abcam, Shanghai, China) for 1 h at room temperature. Protein bands were visualized using the BeyoECL Star Kit (P0958M, Beyotime, Shanghai, China).

Cell counting kit-8 (CCK-8) assay

NB cells were co-cultured with IL-6-silenced PMSCs in a Transwell system for 24 h, then rinsed with PBS and transferred into 96-well plates at a density of 10^4 cells/well. At indicated time points (0, 24, 48, 72 h), $10 \mu L$ of CCK-8 solution (C0038, Beyotime, Shanghai, China) was added to each well and incubated for 4 h at 37°C in the dark. Cell viability was determined by measuring optical density (OD) at 450 nm using a microplate reader.

Colony formation assay

NB cells were first co-cultured with PMSCs, sh-Con, or sh-IL-6 PMSCs in a Transwell system for 24 h, then collected and subjected to 0.25% trypsin digestion. The digested NB cells were adjusted to a concentration of 1×10^6 cells/mL with DMEM medium containing 20% FBS. A

bottom layer of 1.2% agarose (mixed 1:1 with 2 × DMEM medium containing antibiotics) was added to a plate (~7 mL). Then, a top layer of 0.7% agarose (also 1:1 with 2 × DMEM) containing 0.2 mL NB cell suspension was overlaid. After solidification, plates were incubated at 37°C for 14 days, fixed with 4% paraformaldehyde, and stained with 0.1% crystal violet. Colonies containing > 50 cells were counted under an inverted microscope.

Flow cytometry analysis of cell cycle and apoptosis

For cell cycle analysis, NB cells were fixed in 70% cold ethanol overnight at 4°C, washed in PBS, and stained with a solution containing 25 μ L propidium iodide (PI) and 10 μ L RNase A in 0.5 mL staining buffer for 30 min at 37°C in the dark. DNA content was analyzed using flow cytometry and FlowJo 7.6 software.

For apoptosis analysis, NB cells were collected, washed, and resuspended in 100 μ L of 1× binding buffer. Annexin V-PE and 7-AAD (Apoptosis Detection Kit, CA1030, Solarbio, Beijing, China) were added, and cells were incubated for 10 min at room temperature in the dark. After adding 400 μ L of 1× binding buffer, stained cells were analyzed by flow cytometry.

Transwell assay

A Transwell chamber (8 μ m, Corning Inc., Corning, NY, USA) was used to assess NB cell migration and invasion. For the invasion assay, the membrane was pre-coated with Matrigel (M8370, Solarbio, Beijing, China); for migration assays, no coating was applied.

A total of 1×10⁵ PMSCs cells were seeded in the lower chamber and incubated overnight. After 24 h, the insert was gently turned over and inserted into a 6-well plate. Next, NB cells were added to the top chamber at the same density and incubated for 48 h. NB cells were then harvested for migration analysis.

In another setup, 150 μ L PMSCs (1×10⁴) were added to the upper cavity of a 24-well transwell plate with an 8 μ m aperture, using DMEM (without serum) as the medium. Meanwhile, 700 μ L NB cell suspension (1×10⁴) was added into the lower cavity. After incubation at 37°C for 24 h, the bottom of the cavity was washed with PBS, and the upper membrane surface was wiped

Table 1. Primers

Primers	Sequence (5' → 3')	Product lengths
CXCL1-F	AGCTTGCCTCAATCCTGCATCC	119 bp
CXCL1-R	TCCTTCAGGAACAGCCACCAGT	119 bp
GAPDH-F	CCTTCCGTGTCCCCACT	100 bp
GAPDH-R	GCCTGCTTCACCACCTTC	100 bp
CXCL2-F	AACCGAAGTCATAGCCACA	150 bp
CXCL2-R	CAGGAACAGCCACCAATAA	150 bp
CXCL3-F	TTCACCTCAAGAACATCCAAAGTG	94 bp
CXCL3-R	TTCTTCCCATTCTTGAGTGTGGC	94 bp
CXCL6-F	GGGAAGCAAGTTTGTCTGGACC	141 bp
CXCL6-R	AAACTGCTCCGCTGAAGACTGG	141 bp
IL-8-F	GTGCTGTTTGAATTACGGA	64 bp
IL-8-R	TTGACTGTGGAGTTTTGGC	64 bp
IL-32-F	GGGTGAAGGAGAAGGTGGT	120 bp
IL-32-R	GGGCTCCGTAGGACTGG	120 bp

Note: CXCL1, C-X-C motif ligand 1; GAPDH, Glyceraldehyde-3-phosphate dehydrogenase; IL-8, interleukin (IL)-8.

with a cotton swab. Invaded cells were fixed with 4% paraformaldehyde (P0099-3L, Beyotime, Shanghai, China) at 4°C for 20 min. Subsequently, 0.1% crystal violet (0.1%; C8470, Solarbio, Beijing, China) was used to stain the cells for 10 min. The number of invaded cells was observed under a microscope. Each condition was tested in triplicate.

Quantitative real-time polymerase chain reaction (qRT-PCR)

Total RNA was extracted using TriQuick Reagent (W0250, Solarbio, Beijing, China), and cDNA synthesis was synthesized using a cDNA Synthesis Kit (G3333-100, Servicebio, Wuhan, China). qRT-PCR was performed with a 2 × SYBR Green qPCR Master Mix (Low ROX) (G3324-15, Servicebio, Wuhan, China) on a real-time PCR system. Relative gene expression was calculated using the 2-DACT method, with glyceraldehyde-3-phosphate dehydrogenase (GAPDH) as the internal control. Primer sequences are provided in **Table 1**.

RNA-seq

RNA sequencing libraries were constructed following standard protocols, including endrepair, adapter ligation, PCR amplification, and purification. Sequencing was performed on an Illumina platform. Differentially expressed genes (DEGs) were identified using the limma

package in R, with adjusted P < 0.05 and $|log2(Fold\ Change)|$ > 1 as thresholds. Gene Ontology (GO) and Kyoto Encyclopedia of Genes and Genomes (KEGG) pathway enrichment were analyzed using the *ClusterProfiler* package, with P < 0.05 or FDR < 0.05 considered significant enrichment.

Enzyme-linked immunosorbent assay (ELISA)

To quantify IL-6 levels in the culture supernatant of PMSCs, NB cells, and NB cells co-cultured with infected PMSCs, ELISA was performed using a Human IL-6 ELISA Kit (Lianke, Hangzhou, China) following operation manual.

In vivo animal experiments

Fifteen female BALB/c nude mice (4-5 weeks, ~23.6 g) were obtained from the Henan Experimental Animal Center (China) and acclimated for 1 week at 25°C, 60% humidity before experimentation. The mice were kept in a semibarrier system of constant temperature, constant humidity, sterilized feed and water. Each mouse was subcutaneously injected with 5×10⁵ NB cells. When tumor volumes reached ~50 mm³, mice were randomly assigned to three groups: (1) Normal saline group, (2) sh-Con PMSCs group, (3) sh-IL-6 PMSCs.

Mice in the PMSCs groups received intravenous injections of 1×10^6 PMSCs via the tail vein every 4 days, for a total of four doses. The control group received 150 µL normal saline. Tumor length and width were measured every 3 days, and tumor volume was calculated using the formula: V = (length × width²)/2. When the largest tumor diameter approached ~15 mm, mice were euthanized by intraperitoneal injection of pentobarbital sodium (160 mg/kg). Tumors were excised, weighed, and subjected to Western blot and immunohistochemical analysis.

All animal procedures were conducted in compliance with the NIH Guide for the Care and Use of Laboratory Animals and were approved by the Ethics Committee of the Academy of Medical Sciences, Zhengzhou University (No.: ZZU-LAC20250228).

Immunohistochemistry (IHC) assay

Paraffin-embedded tumor tissues were sectioned at a thickness of 4 μm , deparaffinized, and subjected to antigen retrieval in sodium

citrate solution (C1032, Solarbio, Beijing, China). After blocking, sections were incubated overnight at 4°C with the following primary antibodies: Ki-67 (GB111499, Servicebio, Wuhan, China), PCNA (Lot. 10205-2-AP, Proteintech, Wuhan, China), caspase 9 (Lot. db21445, diagbio, Hangzhou, China), and Snail (13099-1-AP, Proteintech, Wuhan, China). The next day, sections were incubated with a secondary antibody (Abcam) for 1 h at room temperature. After DAB color development (P0203, Beyotime, Shanghai, China) and hematoxylin counterstaining, the sections were examined under a microscope, and representative images were captured with appropriate scale bars.

Statistical analysis

Data from at least three independent experiments were expressed as mean \pm standard deviation (SD). Statistical analysis was performed using SPSS 19.0 (IBM, Armonk, NY, USA). Graphs were generated using GraphPad Prism 8 and Adobe Illustrator Artwork 21.0. Differences between two groups were assessed using Student's t-test, while multiple group comparisons were analyzed using one-way ANOVA and repeated-measures ANOVA, followed via Tukey's post hoc test. A *P*-value < 0.05 was considered statistically significant.

Results

Effects of PMSCs on the progression of NB cells

PMSCs were successfully isolated from chorionic villi and characterized by flow cytometry. The cells were positive for CD90, CD105, CD144, and CD166, and negative for HLA-DR and CD14 (Figure 1A). PMSCs cultured alone served as the PMSCs group, and PMSCs cocultured with NB cells (24 h) constituted the experimental group. WB revealed that IL-6 was significantly elevated in PMSCs after co-culture with NB cells (Figure 1B, P < 0.05). To assess the effect of PMSCs on NB cell growth, CCK-8 and colony formation assays demonstrated enhanced NB cell proliferation and increased colony numbers in the co-culture group compared with NB cells alone (Figure 1C, 1D, P < 0.05). Furthermore, flow cytometry showed decreased NB cell apoptosis in co-culture groups, accompanied by an increased S-phase fraction (Figure 1E, 1F, P < 0.05). Additionally, transwell assays indicated that NB cell migration and invasion were notably enhanced under co-culture conditions (**Figure 1G**, **1H**, P < 0.05).

Effects of PMSCs on NB-related proteins and cytokine expression

To further explore the molecular mechanisms underlying PMSC-mediated effects on NB cells, Western blot analysis was conducted. Co-cultured NB cells exhibited increased expression of the proliferation marker PCNA, invasion-related proteins MMP-1 and MMP-7, and EMT markers Snail, N-cadherin, and Vimentin, whereas caspase 9 and E-cadherin were decreased in co-cultured NB cells (**Figure 2A**, P < 0.05).

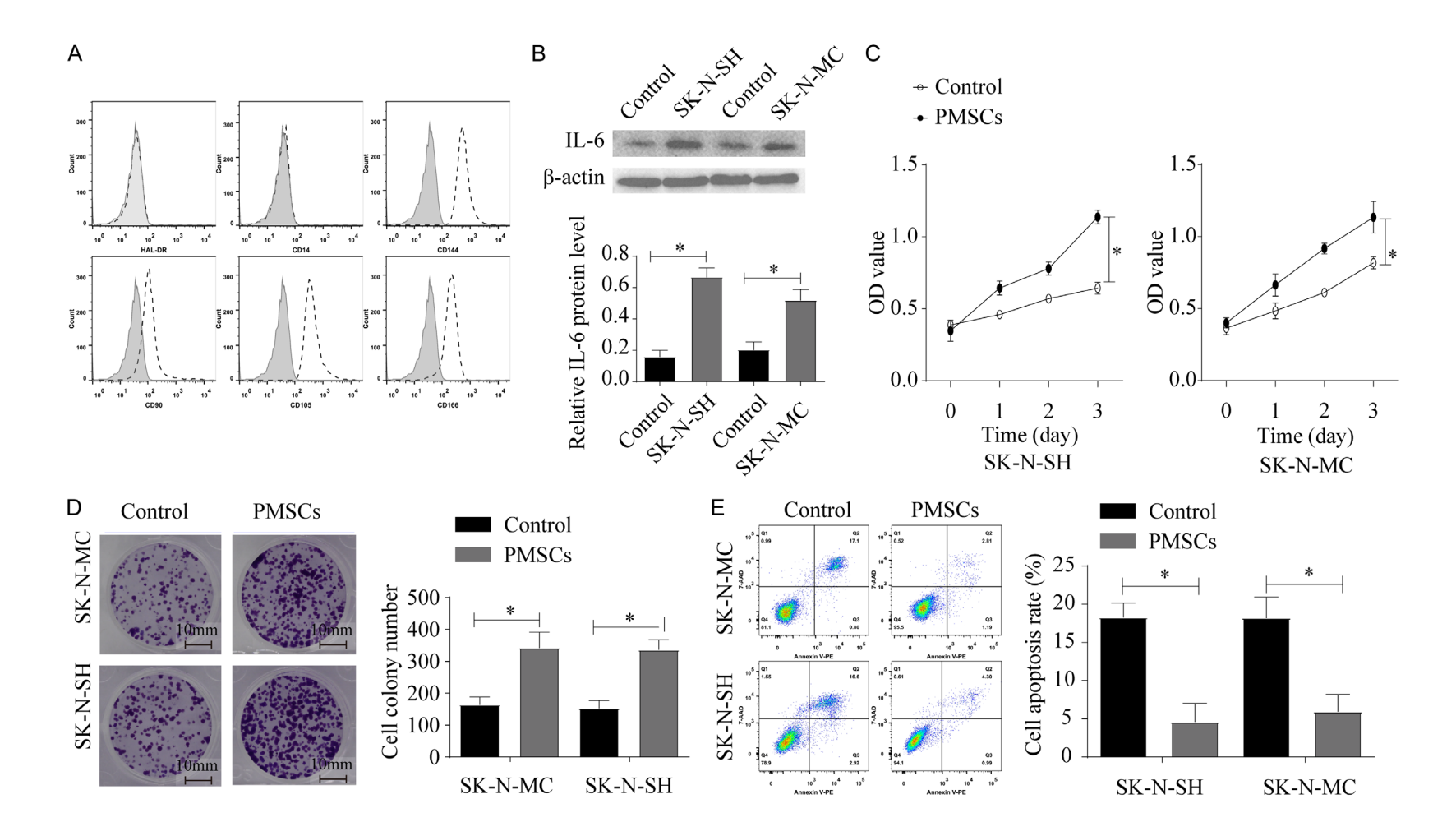
RNA-seq revealed significant upregulation of chemokines including CXCL1, CXCL2, CXCL3, and CXCL6 in NB cells following co-culture (**Figure 2B**, P < 0.05), and qRT-PCR further verified higher levels of IL-8, IL-32, CXCL1, 2, 3, and 6 in co-cultured NB cells (**Figure 2C**, P < 0.05). These findings suggest that PMSCs may promote the malignant behavior of NB cells by upregulating cytokines and activating pathways related to proliferation, invasion, and EMT.

Interference of IL-6 in PMSCs attenuated proliferation, invasion, and promoted apoptosis of NB cells

To determine whether IL-6 is a key mediator of PMSC-induced effects on NB cells, a lentiviral short hairpin RNA targeting IL-6 (sh-IL-6) was constructed and transfected into PMSCs. qRT-PCR confirmed a significant reduction in IL-6 mRNA expression in PMSCs following transfection (**Figure 3A**, P < 0.05). Consistently, WB showed decreased IL-6 protein levels in NB cells co-cultured with IL-6-silenced PMSCs (**Figure 3B**, P < 0.05).

As shown in **Figure 3C**, baseline IL-6 secretion by PMSCs was approximately 10 pg/mL, which was higher than that in NB cells. Co-culture with PMSCs markedly elevated IL-6 levels, while co-culture with IL-6-silenced PMSCs significantly reduced IL-6 concentrations in the supernatant, consistent with the ELISA results (P < 0.05).

CCK-8 and colony formation assay revealed that IL-6 knockdown in PMSCs significantly inhibited NB cell proliferation and colony-forming ability (**Figure 3D**, **3E**, P < 0.05). Flow cytom-



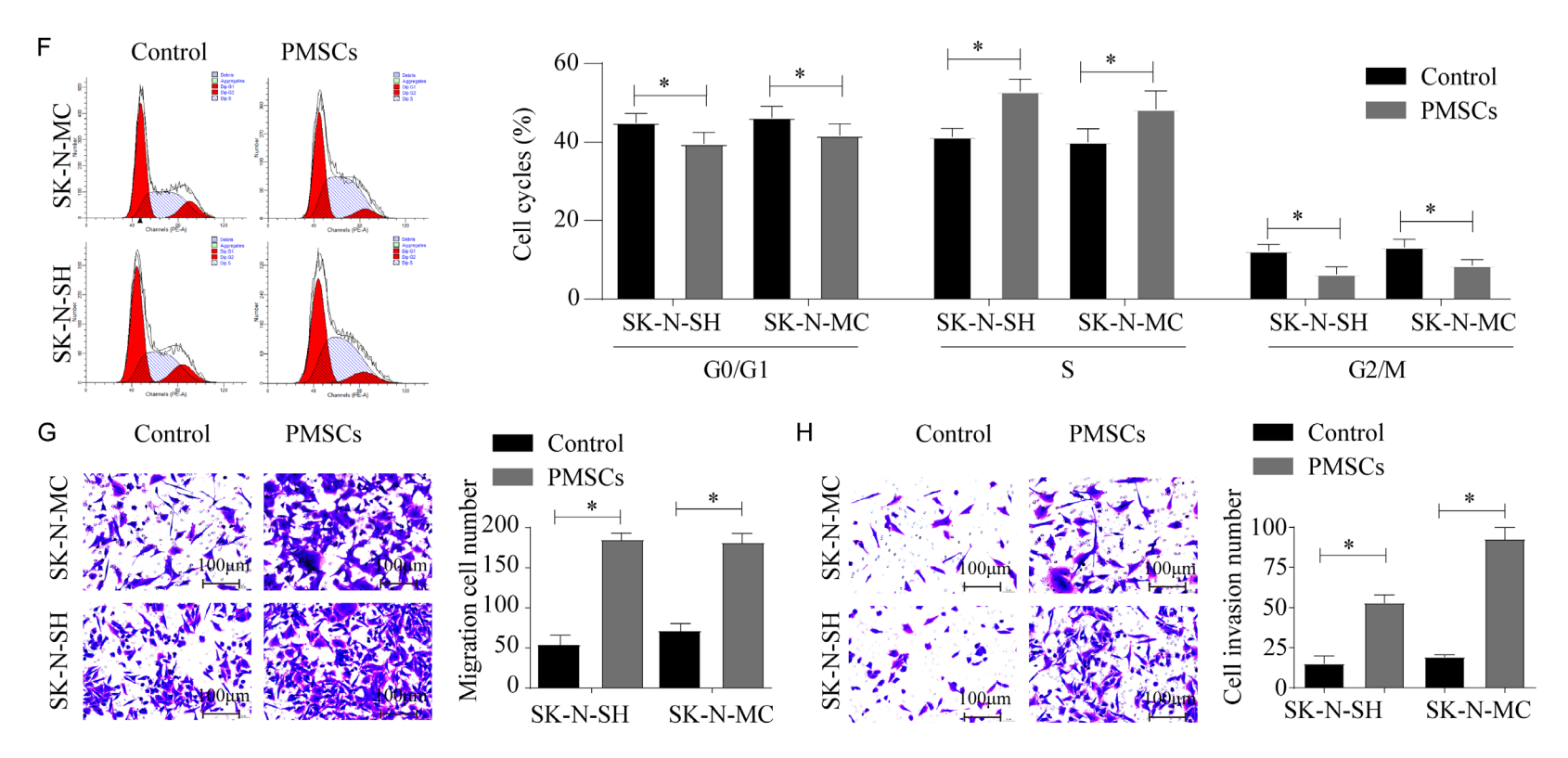


Figure 1. Effects of PMSCs on NB cell progression (SK-N-SH and SK-N-MC). A. Flow cytometry analysis of PMSC surface markers; B. IL-6 expression in PMSCs after co-culture with NB cells, detected by Western blot; C. NB cell viability assessed by CCK-8; D. Colony formation of NB cells; E. NB cell apoptosis detected by flow cytometry; F. Cell cycle distribution detected by flow cytometry; G, H. Migration and invasion detected by Transwell assays (scale bars = $100 \mu m$). n = 6 per group, *P < 0.05. PMSCs, placenta-derived mesenchymal stem cells; NB, neuroblastoma; CCK-8, cell counting kit-8.

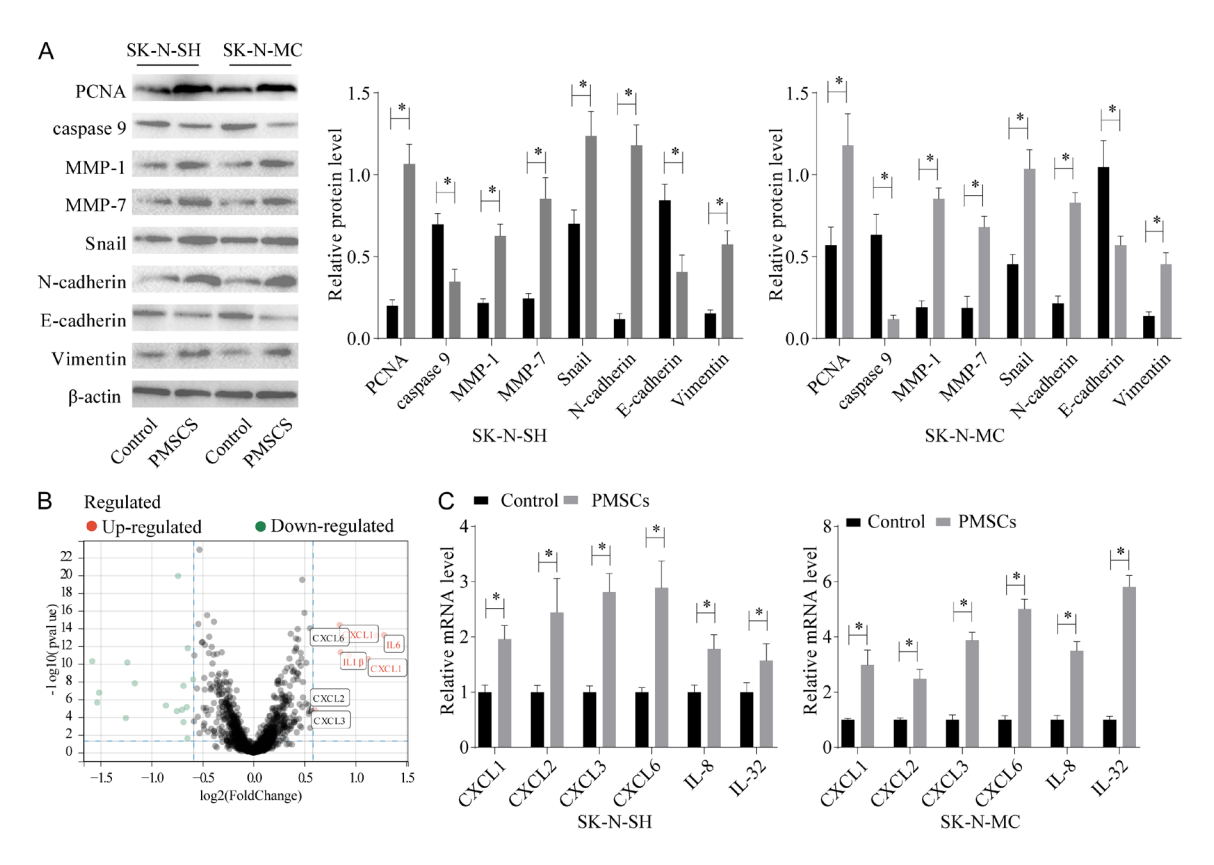


Figure 2. Effects of PMSCs on the expression of growth- and metastasis-related proteins and cytokines in NB cells. A. Western blot analysis of PCNA, caspase 9, MMP-1, MMP-7, Snail, N-cadherin, E-cadherin, and Vimentin in NB cells after co-culture with PMSCs. B. Volcano plot showing differentially expressed genes before and after co-culture of SK-N-SH cells with PMSCs ($|\log 2(FC)| > 1$, adjusted P < 0.05). C. qRT-PCR analysis of IL-8, IL-32, CXCL1, CXCL2, CXCL3, and CXCL6 in NB cells. n = 6 per group, *P < 0.05. PMSCs, placenta-derived mesenchymal stem cells; NB, neuroblastoma; PCNA, proliferating cell nuclear antigen; MMP-1, Matrix metalloproteinase-1; qRT-PCR, quantitative real-time polymerase chain reaction.

etry revealed enhanced NB cell apoptosis and a reduced proportion of S-phase cells, along-side accumulation in the G1/G2-phase (**Figure 3F, 3G,** P < 0.05). Transwell assays further demonstrated that IL-6 interference in PMSCs curtailed NB cell migration and invasion (**Figure 3H, 3I,** P < 0.05), suggesting that IL-6 secreted by PMSCs plays a crucial role in enhancing NB cell malignancy.

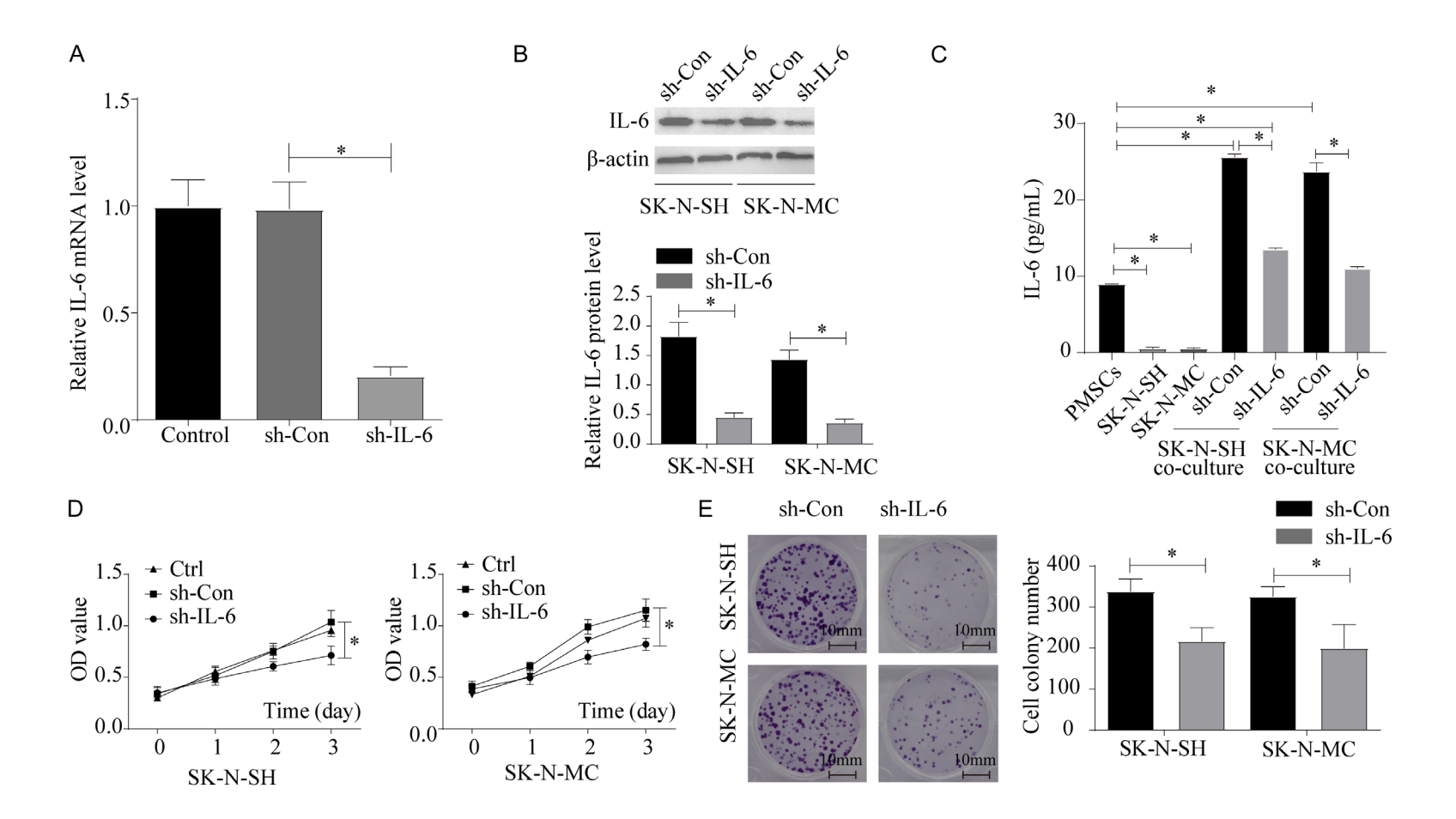
IL-6 silencing downregulated EMT markers and inhibited JAK-STAT/PI3K-AKT signaling in NB cells

RNA-seq analysis of SK-N-SH cells co-cultured with IL-6-silenced PMSCs identified distinct transcriptomic alterations, with 143 genes significantly upregulated and 134 downregulated (Supplementary Table 1). Further KEGG pathway enrichment analysis of the upregulated genes revealed that the JAK-STAT signaling

pathway was significantly enriched in NB cells following co-culture with IL-6-silenced PMSCs (Figure 4A, 4B, P < 0.05). WB showed that the expression of PCNA, MMP-1, MMP-7, Snail, N-cadherin, and Vimentin were notably reduced, while levels of caspase 9 and E-cadherin were elevated in NB cells co-cultured with IL-6-silenced PMSCs (Figure 4C, P < 0.05). Further, the levels of p-JAK2, p-STAT1, p-PI3K, and p-AKT were markedly decreased, while the total protein levels of JAK2, STAT1, PI3K, and AKT remained relatively unchanged (Figure 4D, P < 0.05). These data suggest that IL-6 interference mitigates NB cell progression by suppressing JAK-STAT and PI3K-AKT pathways.

PI3K-AKT pathway inhibition attenuated PMSCs-mediated NB cell growth

To confirm whether the PI3K-AKT pathway mediates PMSCs' tumor-promoting effects, NB



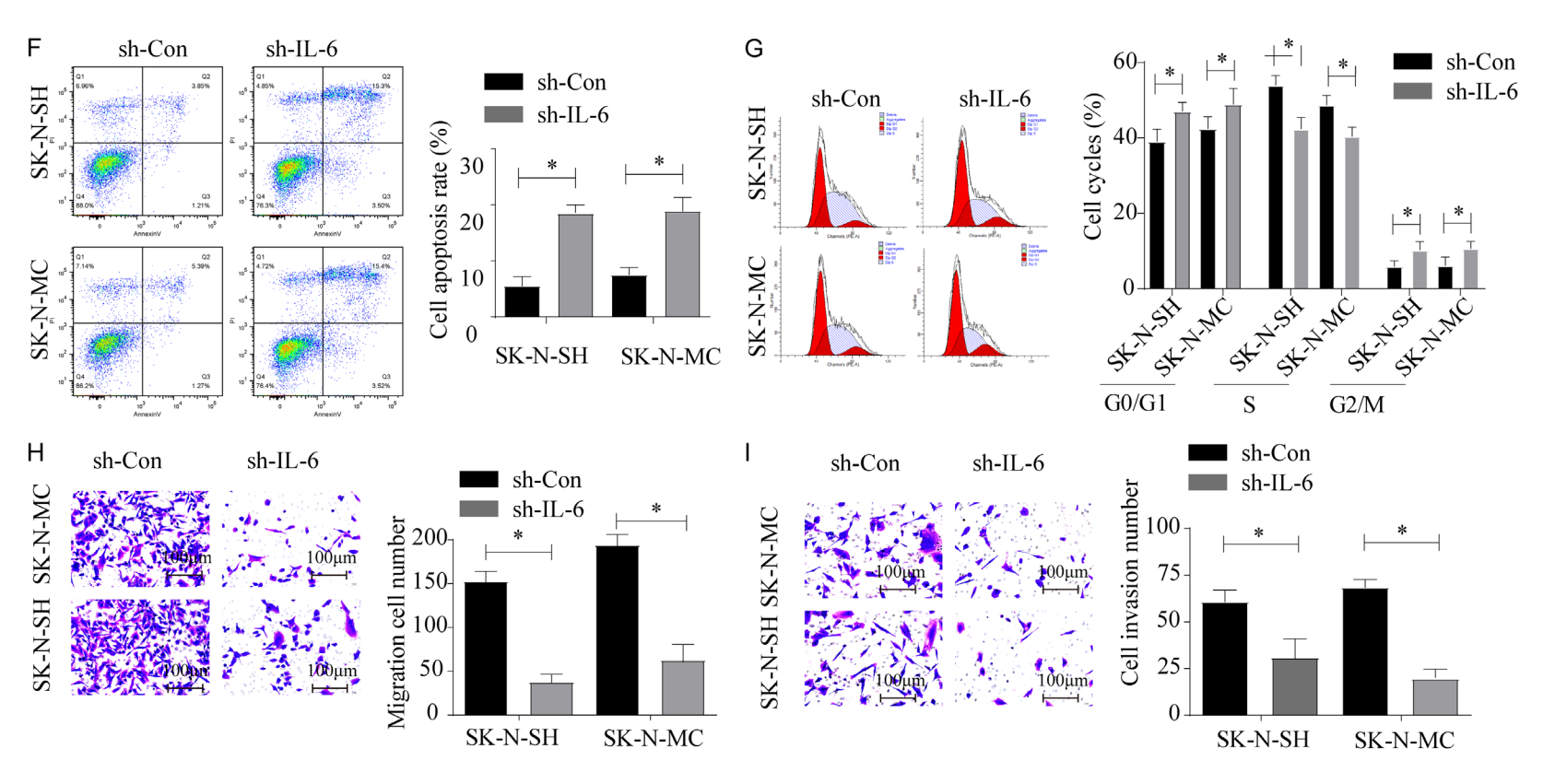


Figure 3. Effects of IL-6 knockdown on proliferation, apoptosis, and invasion of PMSCs-mediated NB cells. A. mRNA expression of IL-6 in PMSCs detected by qRT-PCR; B. Protein expression of IL-6 in PMSCs co-cultured NB cells detected by Western blot; C. IL-6 content in PMSCs, NB cells, and co-culture supernatants detected by ELISA; D. Cell viability of SK-N-SH and SK-N-MC cells detected by CCK-8 assay; E. Effects of IL-6 interference on NB cell clonogenic capacity detected by clone formation assay; F. Effects of IL-6 interference on NB cell cycle distribution; H, I. NB cell migration and invasion detected by Transwell assays (scale bars = 100 μm). n = 6 per group, *P < 0.05. PMSCs, placenta-derived mesenchymal stem cells; NB, neuroblastoma; ELISA, enzyme-linked immunosorbent assay; CCK-8, cell counting kit-8; IL-6, interleukin-6.

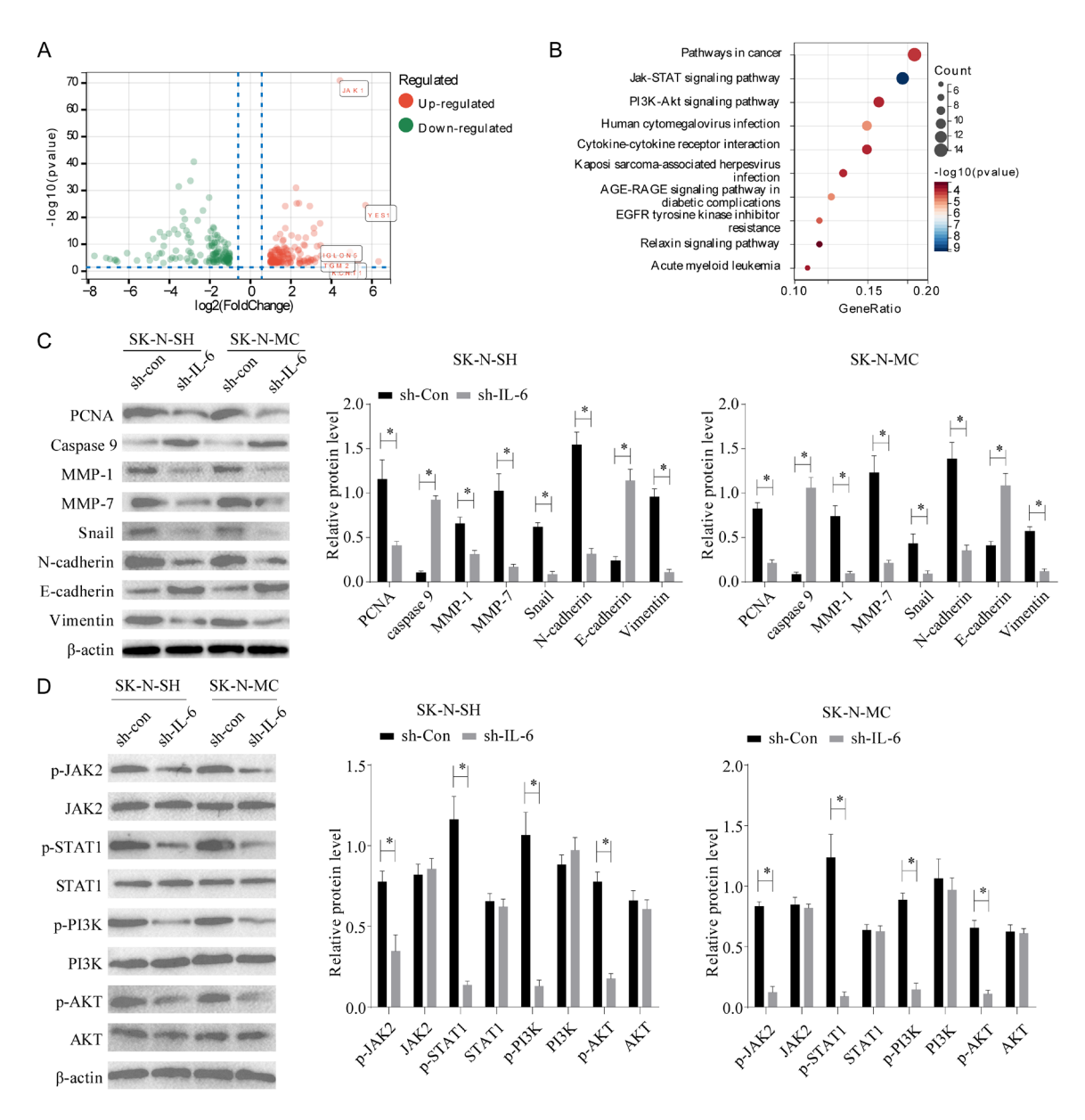


Figure 4. Effects of IL-6 knockdown on proliferation, apoptosis, EMT marker expression, and JAK-STAT/PI3K-AKT signaling in PMSCs-mediated NB cells. A, B. Heatmap of differentially expressed genes (|log2(FC)| > 1, P < 0.05) and KEGG enrichment. C. Western blot analysis of PCNA, caspase 9, MMP-1, MMP-7, Snail, N-cadherin, E-cadherin, and Vimentin. D. Western blot analysis of JAK2, p-JAK2, STAT1, p-STAT1, PI3K, p-PI3K, AKT, and p-AKT. n = 6 per group, *P < 0.05. PMSCs, placenta-derived mesenchymal stem cells; NB, neuroblastoma; EMT, epithelial-mesenchymal transition; JAK/STAT, Janus kinase/signal transducer and activator of the transcription pathways; PI3K/AKT, phosphatidylinositol 3-kinases/protein kinase B; PCNA, proliferating cell nuclear antigen; MMP-1, Matrix metalloproteinase-1.

cells were pretreated with the PI3K inhibitor LY294002 (20 μ M for SK-N-SH and 10 μ M for SK-N-MC, all for 1 h) [22, 23], followed by coculture with PMSCs. CCK-8 assays demonstrated that NB cell proliferation was notably inhibited by LY294002, even in the presence of PMSCs (**Figure 5A**, P < 0.05). Transwell assays showed that LY294002 significantly suppressed NB cell migration and invasion (**Figure 5B**, **5C**, P < 0.05), indicating that PI3K-AKT activation is integral for PMSCs-mediated protumorigenic activity. Western blot confirmed that PI3K, p-PI3K, and p-AKT levels were downregulated in NB cells exposed to LY294002,

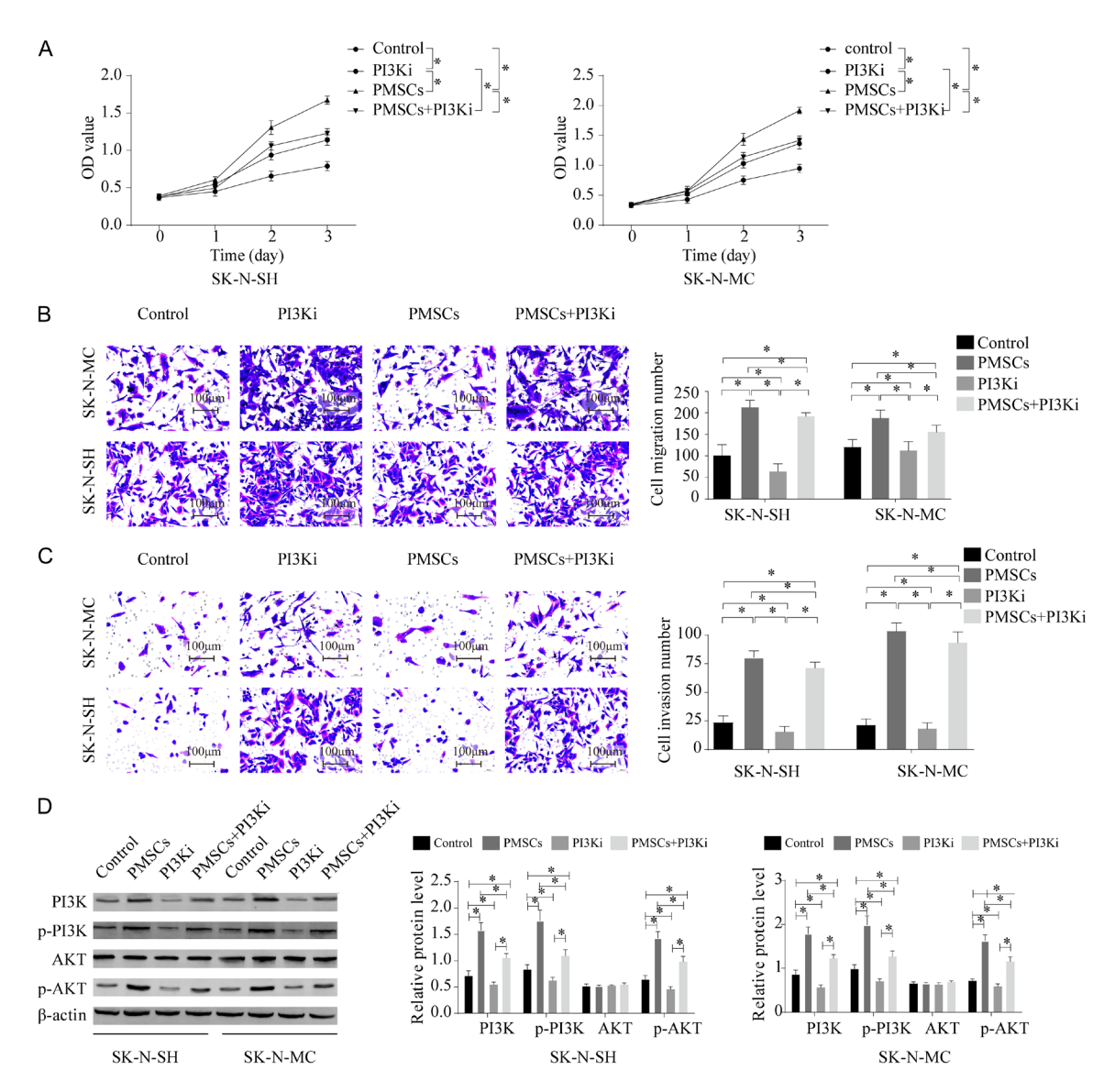


Figure 5. Effects of PI3K inhibitors on PMSCs-mediated NB cell growth and PI3K-AKT signaling pathway. A. CCK-8 assay showing NB cell proliferation treated with or without PI3K inhibitor (LY294002); B, C. Transwell assays for NB cell migration and invasion (scale bars = $100 \mu m$); D. Western blot analysis of p-PI3K, p-AKT, PI3K, and AKT. n = 6 per group, *P < 0.05. PMSCs, placenta-derived mesenchymal stem cells; NB, neuroblastoma; PI3K/AKT, phosphatidylinositol 3-kinases/protein kinase B; CCK-8, cell counting kit-8.

supporting the role of the PI3K-AKT pathway in PMSCs-mediated NB cell growth (**Figure 5D**, P < 0.05).

IL-6 knockdown suppressed PMSCs-mediated NB tumor growth in vivo

To evaluate the in vivo relevance of IL-6 in PMSCs-mediated NB tumor growth, a xenograft model was established. Compared with saline-treated controls, PMSCs significantly increased tumor size and weight, whereas IL-6-silenced PMSCs markedly suppressed tumor growth

(Figure 6A-D, P < 0.05). WB and IHC assays showed elevated expression of IL-6, Ki-67, PCNA, and Snail in tumor tissues from the sh-Con PMSCs group, which was notably reduced in the sh-IL-6 PMSCs group. In contrast, expression of caspase-9 was significantly increased following IL-6 knockdown (Figure 6E, 6F, P < 0.05). Correspondingly, the phosphorylation of JAK2, STAT1, PI3K, and AKT was suppressed by IL-6 knockdown, without substantial changes in total JAK2, STAT1, PI3K, or AKT (Figure 6G, P < 0.05). These results reinforce the notion that IL-6 secreted by PMSCs enhances NB growth *in*

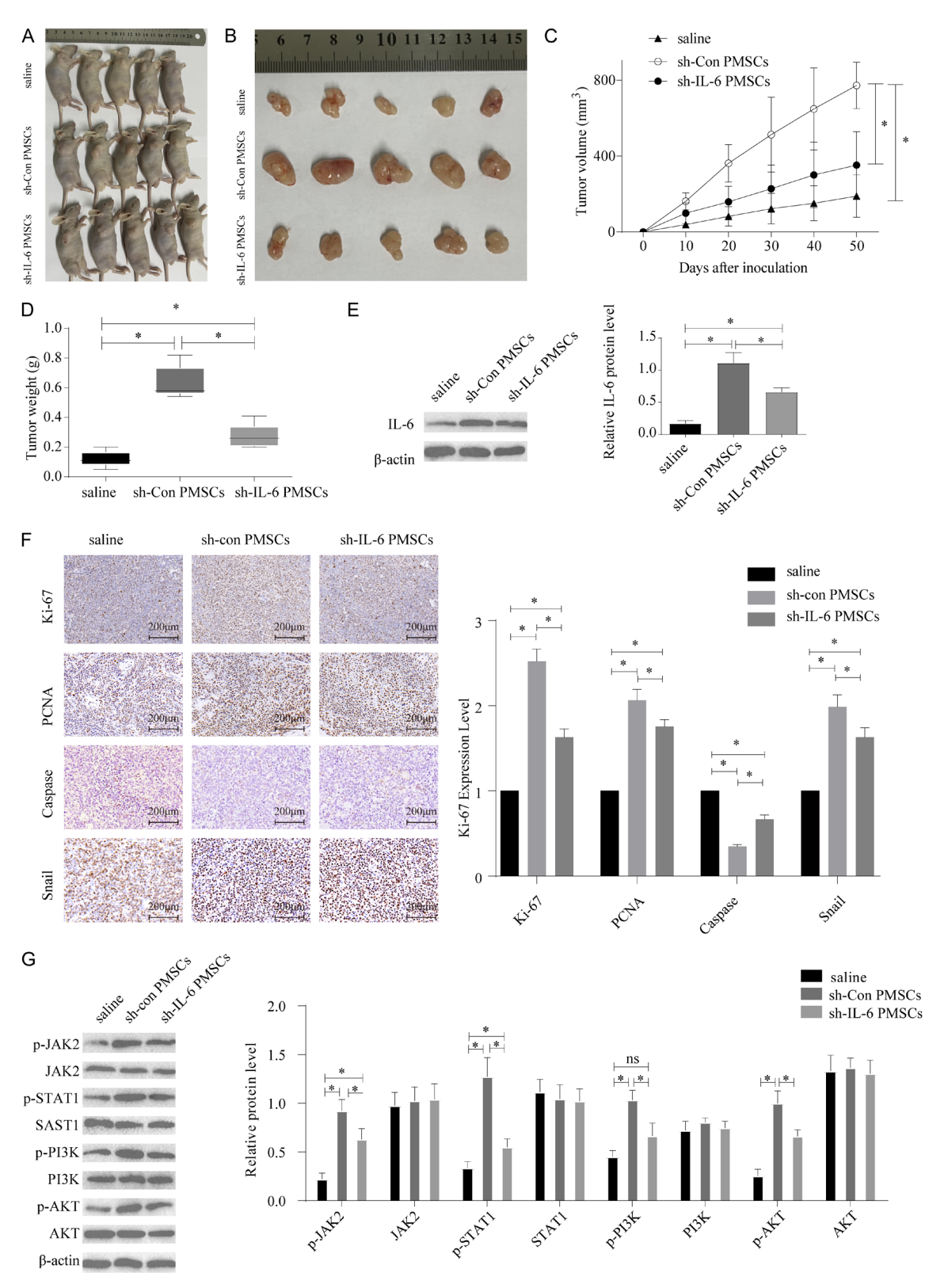


Figure 6. Effects of IL-6 knockdown on NB tumor growth in a xenograft model following PMSCs treatment. A. Tumorbearing nude mice; B. Tumor volume in different groups; C. Tumor growth curves; D. Tumor weights in different groups; E. Western blot analysis of IL-6 expression in tumor tissues; F. Western blot analysis of Ki-67, PCNA, Caspase 9, and Snail in NB-transplanted tumors; G. Western blot analysis of p-JAK2, p-STAT1, p-PI3K, p-AKT, JAK2, STAT1, PI3K, and AKT in tumor tissues. n = 6 per group, *P < 0.05. PMSCs, placenta-derived mesenchymal stem cells; NB, neuroblastoma; IL-6, interleukin -6; JAK, Janus kinase; STAT, signal transducer and activator of the transcription; PI3K, phosphatidylinositol 3-kinases; AKT, protein kinase B; PCNA, proliferating cell nuclear antigen.

vivo, partially via activating JAK-STAT and PI3K-AKT pathways.

Discussion

Neuroblastoma (NB) is a common extracranial tumor in children, accounting for approximately 8% of all pediatric cancers [24-26]. Given the high relapse rates and poor overall survival, there is an urgent need to develop more effective therapeutic strategies for NB. In this study, we investigated the role of placenta-derived mesenchymal stem cells (PMSCs) in NB progression, with a specific focus on IL-6. Our findings revealed that PMSCs significantly increase IL-6 production and other oncogenic cytokines in response to NB cells, thereby enhancing NB cell proliferation, migration, and invasion while suppressing apoptosis.

The role of MSCs in tumor biology remains controversial. Some studies report that MSCs promote tumor growth [27, 28], whereas others suggest an inhibitory effect [29, 30]. This discrepancy may be explained, at least in part, by heterogeneity among MSCs. Previous study has verified that PMSCs from different placental regions display distinct biological behaviors and therapeutic potentials [31]. Consistent with this, our data support the notion that PMSCs can enhance NB malignancy, largely through elevated IL-6 secretion and the subsequent activation of the JAK-STAT and PI3K-AKT signaling pathways.

In our model, SK-N-SH and SK-N-MC cell lines were selected according to previous literatures [32]. Notably, IL-6 level was elevated in NB patients, which served as a poor prognosis in NB progress [33]. We further confirmed that IL-6 knockdown in PMSCs significantly attenuated NB cell proliferation, migration, and invasion. Mechanistically, this was accompanied by decreased phosphorylation of JAK2 and STAT1, as well as downregulation of the PI3K-AKT signaling cascade. This observation is consistent with previous reports implicating IL-6 as a protumorigenic cytokine in various malignancies, including breast and colorectal cancers [34, 35], highlighting its role in promoting tumor cell survival, proliferation, and invasion.

Furthermore, our *in vivo* xenograft experiments confirmed that PMSCs potentiated NB tumor growth, whereas IL-6-silenced PMSCs signifi-

cantly suppressed tumor volume and weight. Notably, both IHC staining and WB analysis demonstrated that Ki-67, PCNA, Snail, and phosphorylated JAK-STAT/PI3K-AKT signaling components were downregulated in tumor tissues from mice treated with sh-IL-6 PMSCs, whereas Caspase 9 was upregulated. However, tumor growth was still enhanced in sh-IL-6 PMSCs group compared to normal saline treated group, suggesting the presence of additional tumor-promoting mechanisms independent of the IL-6 pathway.

Despite these promising findings, several limitations should be acknowledged. First, although IL-6 emerged as a key factor, other PMSCsderived proteins, including MMPs and various cytokines, may also contribute to NB progression. Second, this study primarily focused on the JAK-STAT and PI3K-AKT pathways; however, other signaling cascades, such as MAPK/ERK, may also be involved in PMSCs-NB interactions [36-40]. Third, while the nude mouse xenograft model recapitulates some features of NB tumor biology, it may not fully mirror the complexities of the human tumor microenvironment. Finally, the heterogeneity among PMSCs (e.g., fetal versus maternal sides of the placenta) may influence functional outcomes and should be systematically evaluated in future studies.

In summary, this work indicates that PMSCs promote NB progression by upregulating IL-6 and activating the JAK-STAT/PI3K-AKT signaling pathways. Targeting IL-6 or its downstream pathways may represent an innovative therapeutic strategy for NB, as IL-6 knockdown in PMSCs effectively reduced tumor growth in our xenograft model. Future research should investigate alternative cytokine networks, assess additional signaling pathways, and incorporate more clinically relevant NB models to further advance therapeutic development.

Conclusion

PMSCs promote NB cell proliferation, colony formation, migration, invasion, and epithelial-mesenchymal transition, while inhibiting apoptosis, primarily through upregulation of IL-6 and associated oncogenic cytokines. Silencing IL-6 in PMSCs reduces NB cell growth and tumor progression and enhances apoptosis by inhibiting activation of the JAK-STAT and PI3K-AKT pathways. These findings provide a theoretical

basis for targeting IL-6-mediated signaling in future NB treatments.

Disclosure of conflict of interest

None.

Address correspondence to: Dr. Yufeng Liu, Department of Hematology and Oncology, Children's Hospital, The First Affiliated Hospital of Zhengzhou University, #1, East Jianshe Road, Zhengzhou 450052, Henan, P. R. China. E-mail: 1853857-1287@163.com

References

- [1] Zeineldin M, Patel AG and Dyer MA. Neuroblastoma: when differentiation goes awry. Neuron 2022; 110: 2916-2928.
- [2] Gundem G, Levine MF, Roberts SS, Cheung IY, Medina-Martinez JS, Feng Y, Arango-Ossa JE, Chadoutaud L, Rita M, Asimomitis G, Zhou J, You D, Bouvier N, Spitzer B, Solit DB, Dela Cruz F, LaQuaglia MP, Kushner BH, Modak S, Shukla N, Iacobuzio-Donahue CA, Kung AL, Cheung NV and Papaemmanuil E. Clonal evolution during metastatic spread in high-risk neuroblastoma. Nat Genet 2023; 55: 1022-1033.
- [3] Gomez RL, Ibragimova S, Ramachandran R, Philpott A and Ali FR. Tumoral heterogeneity in neuroblastoma. Biochim Biophys Acta Rev Cancer 2022; 1877: 188805.
- [4] Kennedy PT, Zannoupa D, Son MH, Dahal LN and Woolley JF. Neuroblastoma: an ongoing cold front for cancer immunotherapy. J Immunother Cancer 2023; 11: e007798.
- [5] Liu APY, Dhanda SK, Lin T, Sioson E, Vasilyeva A, Gudenas B, Tatevossian RG, Jia S, Neale G, Bowers DC, Hassall T, Partap S, Crawford JR, Chintagumpala M, Bouffet E, McCowage G, Broniscer A, Qaddoumi I, Armstrong G, Wright KD, Upadhyaya SA, Vinitsky A, Tinkle CL, Lucas J, Chiang J, Indelicato DJ, Sanders R, Klimo P Jr, Boop FA, Merchant TE, Ellison DW, Northcott PA, Orr BA, Zhou X, Onar-Thomas A, Gajjar A and Robinson GW. Molecular classification and outcome of children with rare CNS embryonal tumors: results from St. Jude Children's Research Hospital including the multi-center SJYCO7 and SJMBO3 clinical trials. Acta Neuropathol 2022; 144: 733-746.
- [6] Lundberg KI, Treis D and Johnsen JI. Neuroblastoma heterogeneity, plasticity, and emerging therapies. Curr Oncol Rep 2022; 24: 1053-1062.
- [7] Pieniazek B, Cencelewicz K, Bzdziuch P, Mlynarczyk L, Lejman M, Zawitkowska J and Derwich K. Neuroblastoma-a review of combination immunotherapy. Int J Mol Sci 2024; 25: 7730.

- [8] Croteau N, Nuchtern J and LaQuaglia MP. Management of neuroblastoma in pediatric patients. Surg Oncol Clin N Am 2021; 30: 291-304
- [9] Ahmed AA, Zhang L, Reddivalla N and Hetherington M. Neuroblastoma in children: update on clinicopathologic and genetic prognostic factors. Pediatr Hematol Oncol 2017; 34: 165-185.
- [10] Lan T, Luo M and Wei X. Mesenchymal stem/ stromal cells in cancer therapy. J Hematol Oncol 2021; 14: 195.
- [11] Xie M, Tao L, Zhang Z and Wang W. Mesenchymal stem cells mediated drug delivery in tumor-targeted therapy. Curr Drug Deliv 2021; 18: 876-891.
- [12] Becerril-Rico J, Alvarado-Ortiz E, Toledo-Guzman ME, Pelayo R and Ortiz-Sanchez E. The cross talk between gastric cancer stem cells and the immune microenvironment: a tumorpromoting factor. Stem Cell Res Ther 2021; 12: 498.
- [13] Wu C, Cao X, Xu J, Wang L, Huang J, Wen J, Wang X, Sang X, Zhu W, Yao Y, Zhou C, Huang F and Wang M. Hsa_circ_0073453 modulates IL-8 secretion by GC-MSCs to promote gastric cancer progression by sponging miR-146a-5p. Int Immunopharmacol 2023; 119: 110121.
- [14] Jayaraman H, Ghone NV, Rajan RK and Dashora H. The Role of cytokines in interactions of mesenchymal stem cells and breast cancer cells. Curr Stem Cell Res Ther 2021; 16: 443-453.
- [15] Kavianpour M, Saleh M and Verdi J. The role of mesenchymal stromal cells in immune modulation of COVID-19: focus on cytokine storm. Stem Cell Res Ther 2020; 11: 404.
- [16] Weng Z, Zhang B, Wu C, Yu F, Han B, Li B and Li L. Therapeutic roles of mesenchymal stem cellderived extracellular vesicles in cancer. J Hematol Oncol 2021; 14: 136.
- [17] Chu Y, Liu H, Lou G, Zhang Q and Wu C. Human placenta mesenchymal stem cells expressing exogenous kringle1-5 protein by fiber-modified adenovirus suppress angiogenesis. Cancer Gene Ther 2014; 21: 200-208.
- [18] Hirano T. IL-6 in inflammation, autoimmunity and cancer. Int Immunol 2021; 33: 127-148.
- [19] Antoon R, Overdevest N, Saleh AH and Keating A. Mesenchymal stromal cells as cancer promoters. Oncogene 2024; 43: 3545-3555.
- [20] Oskarsson T, Acharyya S, Zhang XH, Vanharanta S, Tavazoie SF, Morris PG, Downey RJ, Manova-Todorova K, Brogi E and Massague J. Breast cancer cells produce tenascin C as a metastatic niche component to colonize the lungs. Nat Med 2011; 17: 867-874.
- [21] Pelekanos RA, Sardesai VS, Futrega K, Lott WB, Kuhn M and Doran MR. Isolation and expansion of mesenchymal stem/stromal cells

- derived from human placenta tissue. J Vis Exp 2016; 54204.
- [22] Qiao J, Kang J, Ko TC, Evers BM and Chung DH. Inhibition of transforming growth factor-beta/ Smad signaling by phosphatidylinositol 3-kinase pathway. Cancer Lett 2006; 242: 207-214.
- [23] Yoo YM, Jung EM, Ahn C and Jeung EB. Nitric oxide prevents H(2)O(2)-induced apoptosis in SK-N-MC human neuroblastoma cells. Int J Biol Sci 2018; 14: 1974-1984.
- [24] Valter K, Zhivotovsky B and Gogvadze V. Cell death-based treatment of neuroblastoma. Cell Death Dis 2018; 9: 113.
- [25] Khelifa L, Hu Y, Tall J, Khelifa R, Ali A, Poon E, Khelifa MZ, Yang G, Jones C, Moreddu R, Jiang N, Tasoglu S, Chesler L and Yetisen AK. Diagnostic technologies for neuroblastoma. Lab Chip 2025; 25: 3630-3664.
- [26] Irwin MS, Naranjo A, Zhang FF, Cohn SL, London WB, Gastier-Foster JM, Ramirez NC, Pfau R, Reshmi S, Wagner E, Nuchtern J, Asgharzadeh S, Shimada H, Maris JM, Bagatell R, Park JR and Hogarty MD. Revised neuroblastoma risk classification system: a report from the Children's Oncology Group. J Clin Oncol 2021; 39: 3229-3241.
- [27] Frisbie L, Pressimone C, Dyer E, Baruwal R, Garcia G, St Croix C, Watkins S, Calderone M, Gorecki G, Javed Z, Atiya HI, Hempel N, Pearson A and Coffman LG. Carcinoma-associated mesenchymal stem cells promote ovarian cancer heterogeneity and metastasis through mitochondrial transfer. Cell Rep 2024; 43: 114551.
- [28] Ji R, Lin J, Gu H, Ma J, Fu M and Zhang X. Gastric cancer derived mesenchymal stem cells promote the migration of gastric cancer cells through miR-374a-5p. Curr Stem Cell Res Ther 2023; 18: 853-863.
- [29] Tu Z and Karnoub AE. Mesenchymal stem/ stromal cells in breast cancer development and management. Semin Cancer Biol 2022; 86: 81-92.
- [30] Liu QW, Ying YM, Zhou JX, Zhang WJ, Liu ZX, Jia BB, Gu HC, Zhao CY, Guan XH, Deng KY and Xin HB. Human amniotic mesenchymal stem cellsderived IGFBP-3, DKK-3, and DKK-1 attenuate liver fibrosis through inhibiting hepatic stellate cell activation by blocking Wnt/beta-catenin signaling pathway in mice. Stem Cell Res Ther 2022; 13: 224.
- [31] Deng X, Zhang S, Qing Q, Wang P, Ma H, Ma Q, Zhao W, Tang H and Lu M. Distinct biological characteristics of mesenchymal stem cells separated from different components of human placenta. Biochem Biophys Rep 2024; 39: 101739.

- [32] Park MH, Son DJ, Kwak DH, Song HS, Oh KW, Yoo HS, Lee YM, Song MJ and Hong JT. Snake venom toxin inhibits cell growth through induction of apoptosis in neuroblastoma cells. Arch Pharm Res 2009; 32: 1545-1554.
- [33] Moreno-Guerrero SS, Ramirez-Pacheco A, Rocha-Ramirez LM, Hernandez-Pliego G, Eguia-Aguilar P, Escobar-Sanchez MA, Reyes-Lopez A, Juarez-Villegas LE and Sienra-Monge JJL. Association of genetic polymorphisms and serum levels of IL-6 and IL-8 with the prognosis in children with neuroblastoma. Cancers (Basel) 2021; 13: 529.
- [34] Siersbaek R, Scabia V, Nagarajan S, Chernukhin I, Papachristou EK, Broome R, Johnston SJ, Joosten SEP, Green AR, Kumar S, Jones J, Omarjee S, Alvarez-Fernandez R, Glont S, Aitken SJ, Kishore K, Cheeseman D, Rakha EA, D'Santos C, Zwart W, Russell A, Brisken C and Carroll JS. IL6/STAT3 signaling hijacks estrogen receptor alpha enhancers to drive breast cancer metastasis. Cancer Cell 2020; 38: 412-423. e9.
- [35] Lin T, Zhang S, Tang Y, Xiao M, Li M, Gong H, Xie H and Wang Y. ART1 knockdown decreases the IL-6-induced proliferation of colorectal cancer cells. BMC Cancer 2024; 24: 354.
- [36] Zhou F, Li YH, Wang JJ, Pan J and Lu H. Endoplasmic reticulum stress could induce autophagy and apoptosis and enhance chemotherapy sensitivity in human esophageal cancer EC9706 cells by mediating PI3K/Akt/ mTOR signaling pathway. Tumour Biol 2017; 39: 1010428317705748.
- [37] Ouyang J, Pan X, Lin H, Hu Z, Xiao P and Hu H. GKN2 increases apoptosis, reduces the proliferation and invasion ability of gastric cancer cells through down-regulating the JAK/STAT signaling pathway. Am J Transl Res 2017; 9: 803-811.
- [38] Ke F, Wang Z, Song X, Ma Q, Hu Y, Jiang L, Zhang Y, Liu Y, Zhang Y and Gong W. Cryptotanshinone induces cell cycle arrest and apoptosis through the JAK2/STAT3 and PI3K/Akt/ NFkappaB pathways in cholangiocarcinoma cells. Drug Des Devel Ther 2017; 11: 1753-1766.
- [39] Kaya Y, Kucukvardar S and Yildiz A. Speedy/ RINGO protein interacts with ERK/MAPK and PI3K/AKT pathways in SH-SY5Y neuroblastoma cells. Mol Cell Biochem 2020; 473: 133-141.
- [40] Yu X, Fan H, Jiang X, Zheng W, Yang Y, Jin M, Ma X and Jiang W. Apatinib induces apoptosis and autophagy via the PI3K/AKT/mTOR and MAPK/ERK signaling pathways in neuroblastoma. Oncol Lett 2020; 20: 52.